Role of Transition Metal Oxides in Metal Dusting: Density Functional Study

Hansong Cheng, David B. Reiser, Paul M. Mathias, and Sheldon Dean, Jr.
Air Products and Chemicals, Inc., Allentown, PA 18195

Density function theory was applied to study the mechanisms and energetics of two major metal dusting processes represented by Boudouard and steam-carbon reactions on the FeO(100) surface. Cluster models were utilized to represent the surface. The chosen cluster model was validated by examining CO adsorption binding energies on clusters of various sizes. We show that the lattice relaxation has a relatively small effect on the adsorption. The reaction process involving direct abstraction of O from the surface by CO was excluded from consideration of the overall dusting processes due to unfavorable energetics. Minimum energy path calculations were carried out to investigate the reaction mechanisms. It was found that both the Boudouard and steam-carbon reactions are thermochemically and kinetically unfavorable on transition metal oxide surfaces. Detailed insight into the reaction mechanisms was obtained by following the reaction trajectories and analyzing the electron population distribution along the reaction paths. This study elucidates the empirical observation that metal oxide can often minimize metal dusting.

Introduction

There have been several recent efforts that used first-principles electronic structure methods to study chemical reactions and molecular chemisorption and/or physisorption at solid surfaces (Hammer et al., 1993; Hammer and Nørskov, 1995; Neurock et al., 1994). The development was primarily motivated by potential applications to heterogeneous catalysis. Many studies have demonstrated that quantum-mechanical calculations are capable of unraveling the detailed mechanisms that govern gas-solid interaction processes (Hammer et al., 1995; Neurock et al., 1994; Jansen et al., 1988; van Daelen et al., 1996). Coupled with sophisticated spectroscopic techniques, these calculations can now provide quantitative or semiquantitative information about the energetics adsorption structures and electronic configurations of molecular species at surfaces. These developments have been summarized in several reviews (van Santen et al., 1995; Ellis et al., 1991; Feiblman, 1994; van Santen, 1991).

Corrosion is an important industrial problem. While much theoretical effort has been concentrated on heterogeneous catalysis, application of electronic structure methods to chemical corrosion at solid surfaces has been largely neglected. The fundamental difference between the catalytic reactions and chemical corrosion on surfaces lies in the fact that ideally the surfaces remain "clean" before and after the reactions in a catalytic process; in a corrosion system, however, the solids are often heavily involved in surface reactions in which the gas species may deposit on the surfaces and the solid materials are eventually degraded. In spite of the difference, the theoretical methods effectively utilized in heterogeneous catalysis should also be useful for studies on corrosion phenomena at solids. We have recently applied first-principle calculations to understanding the mechanisms of nitriding at metal surfaces (Cheng et al., 1995, 1996). We showed that much insight can be gained by examining the energetics and structures of the nitriding species. In this article, we report our density functional studies on another important corrosion process: dusting at metal oxide surfaces. The goal of this work is to understand the role of metal oxide components in stainless steels in the dusting process.

Metal dusting is a detrimental corrosion phenomenon at high temperature (400 – 800°C) that occurs in many industrial processes such as synthesis gas production, coal gasification, and iron ore reduction (Davis et al., 1953; Walker et al., 1959; Hoyt et al., 1959; Richardson, 1993; Grabke et al., 1993a,b). Alloys that contain Ni, Fe, Co, and Cr are susceptible to metal dusting. As a consequence, these materials are disintegrated

Correspondence concerning this article should be addressed to H. Cheng.

into fine particles of metals, metal oxides and carbides, etc. It is generally believed that the corrosive processes involve chemisorption of carbon monoxide at alloy or stainless steel surfaces and subsequent deposition of carbon on these materials resulting from the interaction between the adsorbed species and the gas streams through the Boudouard and steam-carbon reactions. These two reactions are, respectively, described by the following processes:

$$CO + CO \rightarrow C + CO_2,$$

$$CO + H_2 \rightarrow C + H_2O.$$

Preventing metal dusting in industrial processes is essential to achieving high economic efficiency and has presented a great challenge in materials science community. While intensive empirical research effort has been focused on the performance and development of a wide variety of materials that resist carburization and creep, very little is understood about the underlying mechanisms that dictate the dusting processes (Grabke et al., 1993). Quantum-mechanical calculations are capable of unraveling some of the detailed fundamental processes that take place in metal dusting.

Given the fact that both the Boudouard and steam-carbon reactions in the gas phase are extremely unfavorable energetically, surfaces of stainless steels and alloys must play a key role in catalyzing the reactions. Many practical observations suggest that transition metal oxide contents in the stainless steels or alloys significantly minimize dusting, but the fundamental reasons remain unknown. Metal oxides such as FeO and NiO are generally present on stainless-steel surfaces. Understanding the dusting mechanisms at the metal oxide surfaces is certainly an essential step toward understanding the dusting phenomena on materials used in practical processes. Calculations on metal dusting on metal oxides allow us to identify some of the key components that are responsible for the corrosion. Dusting on pure transition metals and alloys is currently under investigation.

The theoretical models used in our calculations and the computational details are described later. Density functional theory (DFT) is utilized throughout this work (Labanowski et al., 1991), and its calculated results are presented. DFT, which has recently been widely applied to electronic structure calculations for systems that contain transition metals, has been proven to be particularly effective in providing a wealth of information about molecular structure and energetics (van Daelen et al., 1996; Ziegler, 1991; Cheng et al., 1996). We will focus on two of the most important dusting processes on transition metal oxide surfaces in this article: Boudouard reaction and carbon-steam reaction. Both reactions involve adsorption and dissociation of CO on surfaces and deposition of C atoms to the surfaces. These reactions are stimulated by interacting with the gas species, such as CO and H_2. We will examine the detailed mechanisms of the reactions as well as the adsorption structures and energetics.

Theoretical Models and Computational Methods

This work utilizes clusters models to describe the metal oxide surfaces. Many studies have showed that carefully selected surface clusters are capable of modeling molecular adsorption phenomena on surfaces (van Daelen et al., 1996; Siegbahn et al., 1992; Estiu et al., 1994; Mijoule et al., 1991). In choosing appropriate clusters for theoretical calculations, two important concerns are taken into account. First, the adsorption binding energies of the gas species must be approximately invariant as the cluster size increases. To model bimolecular reactions on surfaces, the clusters usually must be large enough to accommodate all the reaction species without introducing artifacts in the calculations. This frequently imposes great computational difficulties. Since for the Boudouard and carbon-steam reactions the adsorbed CO interacts with gas-phase CO and H_2, we only need to examine the cluster sizes based on CO adsorption binding energies. The interaction between any adjacent absorbates is neglected. Second, lattice relaxation upon CO adsorption and dissociation can be an important factor that affects the computational accuracy. To avoid artifacts, large surface clusters must be used and geometry optimization schemes need to be carefully chosen. This study deals with the dusting reaction at the FeO(100) surface. Similar calculations were also performed for dusting on the NiO(100) surface and the results will be presented elsewhere.

Our calculations were carried out by using density functional theory under both local spin density (LSD) and nonlocal spin density (NLSD) approximations (Labanowski et al., 1991). The LSD calculations employ the Vosko-Wilk-Nusair local correlation functional, and the NLSD calculations utilize Becke's gradient-corrected exchange functional and Perdew-Wang's gradient-corrected correlation functional (Vosko et al., 1980; Becke, 1983; Perdew et al., 1992). The nonlocal correction was incorporated in the SCF cycles in an iterative manner. Double numerical basis set augmented with polarization functions was utilized, and all inner core electrons were frozen. Our numerical tests suggested that the frozen-core approximation does not significantly affect the computational accuracy. A spin polarized computational scheme was used throughout to deal with the electronically open-shell system. Point group symmetry was imposed whenever applicable in the geometry optimizations to simplify the calculations. All the calculations were performed by using the DMol package (DMOL, v2.3.6, 1994).

Results and Discussions

Cluster sizes

We first examine the effect of cluster size on the CO adsorption binding energy. We thus calculated the adsorption structure of CO on various sizes of clusters of the FeO(100) surface. Many studies showed that CO adsorbs preferably at the "on-top" position of metal atoms in transition metal oxides with the carbon atom toward the surfaces (Yates, Jr., 1994; Kobayashi et al., 1989). Our optimized adsorption geometry, in which CO is adsorbed atop on the center Fe atom, indeed agrees with the result. Figure 1 displays two different sizes of clusters on which CO is adsorbed. The adsorption on top of the central Fe atom was calculated without lattice relaxation. The structures of the chosen surface models and the clusters with adsorption/reaction species exhibit a C_{4v} symmetry. The calculated binding energies and the structural parameters of CO adsorption on these clusters are shown in Table 1. The overbinding of the LSD calculation is corrected

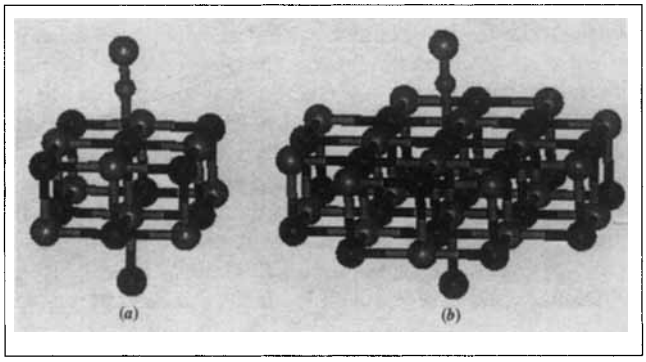

Figure 1. Cluster models of FeO(100) surface.

The geometry optimization was done at the NLSD level. Here CO is adsorbed atop on a Fe atom.

largely in the NLSD calculation, as expected. The calculated CO binding energies on these clusters remain approximately the same. This suggests that the surface effect on adsorption is highly localized around the adsorption site, as expected for a solid with highly covalent bonds like FeO. Therefore, structure a in Figure 1 is appropriate to serve as a surface model since it is relatively small and thus computationally easy to handle. The subsequent reaction of the absorbate with the gas-phase CO and H_2 is not expected to be affected significantly by the relatively small size of the cluster in view of the large distances between these gas species and the surface.

Surface relaxation

The FeO(100) surface was initially constructed from the 3-D crystal structure. The atoms in the top layers of the surface will therefore slightly adjust their positions to respond to the lattice change. Further relaxation of the top layer atoms is expected to occur on CO adsorption and dissociation. To study the lattice relaxation effect on dusting, we used a 43-atom FeO cluster and optimized both the cluster structure and the cluster with an adsorbed CO on top of the central Fe atom in three different optimization schemes. As shown in Figure 2, the first scheme is to optimize only the adsorbate with all the surface atoms frozen, the second one is to optimize the adsorbate and all the surface atoms except the atoms at edges and corners, and the third one extends the optimization to eight additional corner atoms. The main optimized adsorption geometric parameters and binding energies are shown in Table 2 (detailed geometric parameters are available on request). Figure 2 shows that optimizations involving corner and edge atoms significantly distort the lattice structure, which will inevitably result in artifact in calculations. This is further evidence by the much larger CO adsorption

Table 1. Calculated NLSD CO Adsorption Binding Energy ΔE on Clusters in Figure 1 and Main Optimized Bond Parameters

Structure	ΔE (kcal/mol)	C-O (Å)	C-Fe (Å)
a	−7.815	1.169	1.787
b	−7.963	1.172	1.794

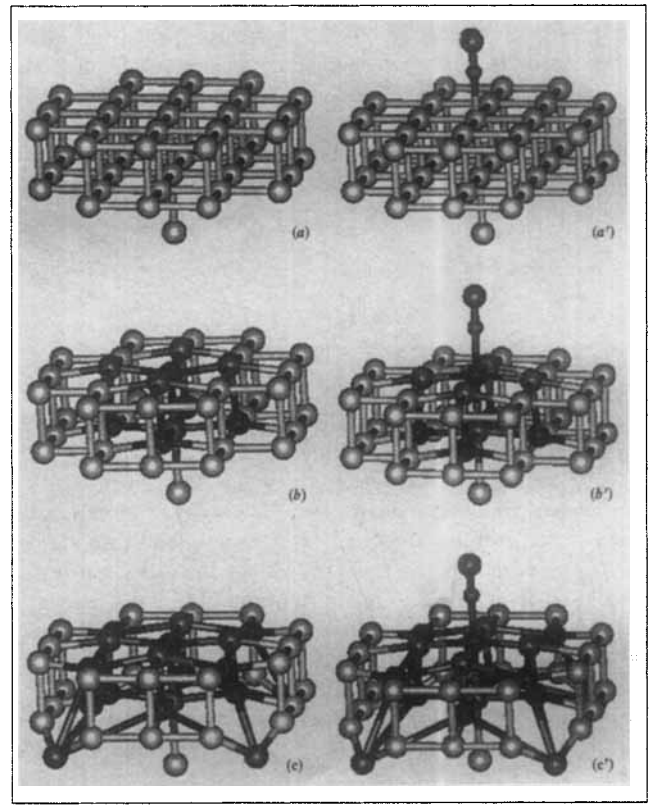

Figure 2. Clusters used for lattice relaxation.

The geometry was optimized at the NLSD level: (a) optimization only on the adsorbate; (b) optimization on the adsorbate and on the surface atoms highlighted by the gray (O atoms) and black (Fe atoms) colors (the white balls represent the surface atoms frozen in their crystal positions), (c) further optimization including the 8 atoms at the corners.

binding energy on the relaxed structure. The second optimization scheme also yields considerable perturbation on the lattice atoms around their positions in crystal structure with O atoms moving slightly out the plane and Fe atoms being slightly imbedded in the surface. However, each of the atoms being optimized is fully surrounded by neighboring atoms and thus the cluster will not be significantly distorted. Upon CO adsorption, the central Fe atom moves up slightly toward the adsorbate, as expected. The CO adsorption binding energy on the partially optimized cluster is only about 2 kcal/mol higher than that on the rigid cluster. We thus conclude that lattice relaxation is not a significant process for dusting at transition metal oxide surfaces. Therefore, in the rest of the article, we will use only structure a in Figure 1 to represent the FeO(100) surface for CO adsorption and dissociation on top of the Fe atom under the rigid lattice approximation.

Table 2. Calculated CO Adsorption Binding Energy ΔE on Clusters in Figure 2 and Main Optimized Bond Parameters*

Structure	ΔE (kcal/mol)	C-O (Å)	C-Fe (Å)
a	−7.963	1.172	1.794
b	−11.407	1.180	1.784
c	−13.832	1.175	1.776

*The optimization was done at the NLSD level.

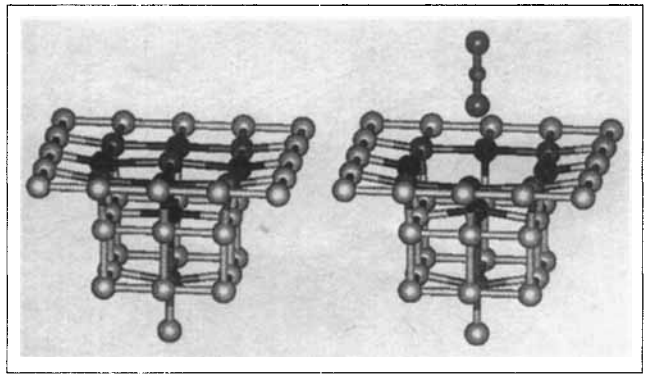

Figure 3. Cluster model used to represent the abstraction process by CO.

Geometry optimization was done at both LSD and NLSD levels. The atoms highlighted in the same fashion as in Figure 2 are included in the geometry optimization.

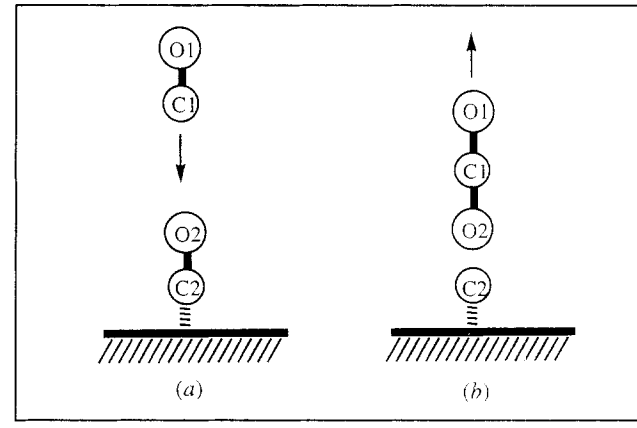

Figure 4. Reaction path calculations for Boudouard reaction for normal incidence.

It has been suggested that CO may extract an O atom from TiO_2 surfaces to form CO_2 (Göpel et al., 1983). We performed geometry optimization for CO to react with the O atom on an FeO(100) cluster. The optimized cluster and CO adsorption geometries are shown in Figure 3. The calculated energy required to extract the O atom from the FeO(100) surface is 22.4 kcal/mol at the LSD level. The extraction energy is expected to be even higher at the NLSD level. Therefore, this is an energetically unfavorable process, although it is interesting to see that the CO_2 is indeed formed. The extraction of an O atom from the surface creates a large hollow; the adjacent Fe atoms move further away from the extracting center to form stronger bonding with the neighboring O atoms instead of forming a closed-packed Fe cluster imbedded in the surface. Therefore, we conclude that CO does not directly interact the O atoms on the surface.

Boudouard reaction

There are several possible channels for the adsorbate to interact with other gas species near or on the FeO(100) surface that may lead to Boudouard reaction. The adsorbate-adsorbate interaction is not expected to be the process that contributes significantly to these reactions in view of the relatively large separation between the adsorbates (about 3.06 Å), the head-on adsorption pattern and, more importantly, very unfavorable orbital overlap. We thus ruled out such a mechanism for dusting on the FeO(100) surface and focus on the processes that involve interactions between adsorbate and gas-phase species.

We first consider the attack on the adsorbate by CO from the surface normal. This allows us to impose a C_{4v} symmetry in the calculation. The gas-phase species approach the adsorbate, forming CO_2 and H_2O and leaving the surface C deposited on the Fe atom. To describe this process, we performed minimum energy path calculations to follow the reaction trajectories, using the procedure in Figure 4. Specifically, for the Boudouard reaction, the gas-phase CO first attacks the adsorbate with the C atom head-on toward the surface (forward reaction); it picks up the O atom from the adsorbate and bounces back to the gas phase (backward reaction). In the forward reaction the distance between the gas-phase C atom and the surface plane serves as the reaction coordinate, while in the backward reaction the bond length of the adsorbate serves as the reaction coordinate. All other degrees of freedom of the molecular species are optimized under the imposed C_{4v} symmetry and the rigid lattice approximation.

Figure 5 displays the calculated energy profile along the minimum energy path of normal incidence for the Boudouard reaction. Geometry optimization was done only at the LSD level. The NLSD energy was calculated using the geometries obtained in the LSD calculations. In essence, the LSD and NLSD results agree with each other. The calculation suggests that the reaction thermo chemistry at the FeO(100) surface is energetically unfavorable. In particular, the activation barrier is exceedingly high. Qualitatively, this conclusion is consistent with the observation that metal oxide surfaces tend to block dusting (Koszman, 1973; Kane, 1986). The calculation has unraveled the fundamental reason behind this phenomenon.

Figure 6 displays the collected bond parameter changes along the reaction coordinate. Figure 6a shows the distance of the C atom of the gas-phase CO from the surface. As the bond distance reaches 4.12 Å, the gas-phase CO arrives at the transition state. It then picks the O atom from the adsorbate to form CO_2, which subsequently goes back to the gas phase. Figure 6b depicts the bond distance between the C atom of the adsorbate and the Fe atom on which CO is adsorbed. The adsorbate is compressed by the incoming CO toward the surface until the reaction arrives at the transition state at which it bounces back. As CO_2 leaves the surface, the deposited C atom slightly stretches its bond with the surface and reaches the optimal bond distance. The change of the bond distance between the gas-phase C atom and the O atom of the adsorbate is shown in Figure 6c. The two atoms gradually form a double bond, which remains steady after the transition state. On the other hand, the bond length of the gas-phase CO stretches from the triple bond distance to the double-bond one, as shown in Figure 6d. Finally, the bond length of the adsorbate is elongated and eventually dissociated along the minimum energy path (Figure 6e).

It is important to examine the charge transfer processes in the gas-surface interface along the reaction pathway to fully understand why metal oxides are dusting-resistant. In Figure

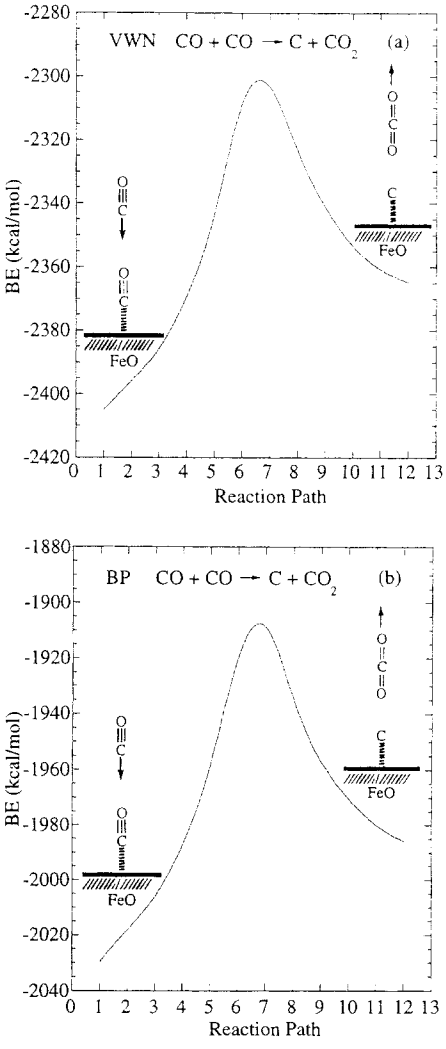

Figure 5. Energy profiles along the reaction coordinate of Boudouard reaction calculated at: (a) LSD and (b) NLSD levels.

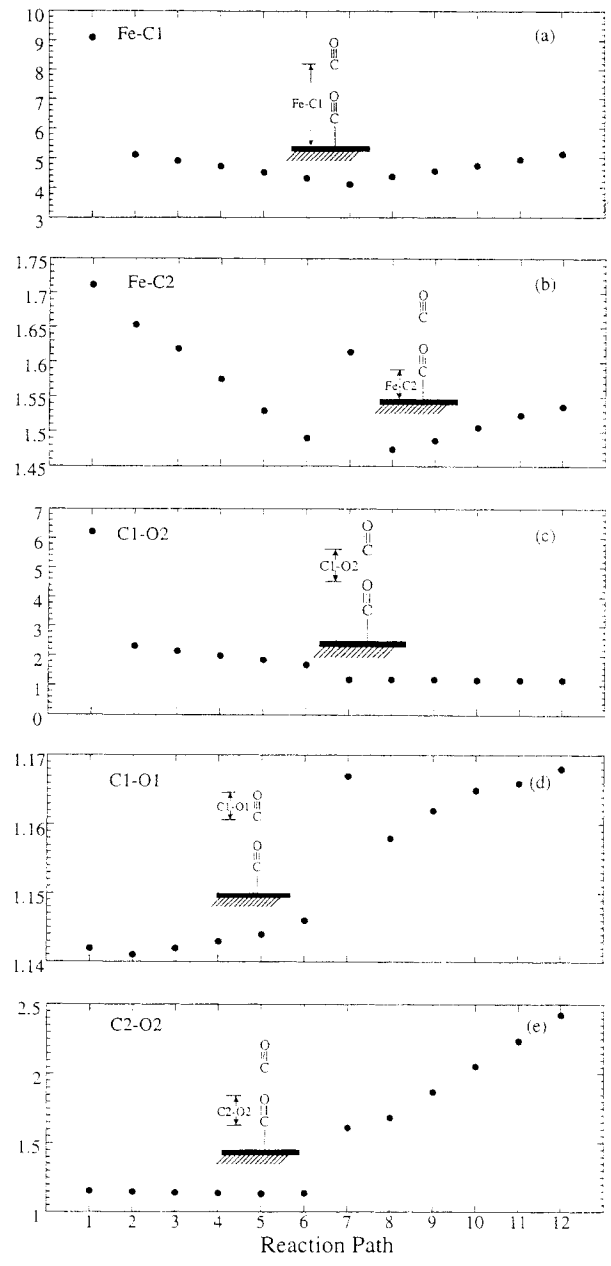

Figure 6. Structural changes along the reaction path for normal incidence.

(a) Distance between the C atom of the gas-phase CO and the surface; (b) bond distance between the C atom of the adsorbed C and surface; (c) distance between the C atom of the gas-phase CO and the O atom of the adsorbed CO; (d) C-O bond distance of the gas-phase CO; (e) C-O bond distance of the adsorbed CO.

7, we show the calculated Mulliken gross charges and the individual atomic charges of the reaction species. Figure 7a shows that the gross charges of the reaction species in the entire reaction process are positive. These charges represent the amount of overall charge transferred to the surface. The charge transfer increases near the transition state and rapidly diminishes with the formation of CO_2. The gross charge variation of the reaction species can be further analyzed in detail by examining the individual atomic charges of the reaction species, as shown in Figure 7b. First, the charge of the C atom of the adsorbate (C2) increases monotonically along the reaction path, because the dissociation of the adsorbate results in much stronger bonding between the C atom and the surface (the calculated NLSD bonding energy of C on the surface is -82.22 kcal/mol). As a consequence, electron donation from the adatom to the surface increases. Second, the small negative charges on the two O atoms of the reaction species are mainly due to the triple-bond nature of CO and they converge to the same value as CO_2 is formed as expected. The maximum charge transfer to the surface observed in Figure 7a is the overall consequence of stronger bonding of adatom-surface and the electron withdrawing effect from the gas-phase O atom to the surface bridged by the O atom of the adsorbate, as seen in Figure 7b. The population analysis suggests that the O atoms in the oxides prompt the metals in a relatively higher oxidation states and thus reduce the tendency of electron back donation. This is in fact consistent with the relatively small CO adsorption energy. As a consequence, the C-O bond becomes strengthened, which prevents Boudouard reaction from occurring.

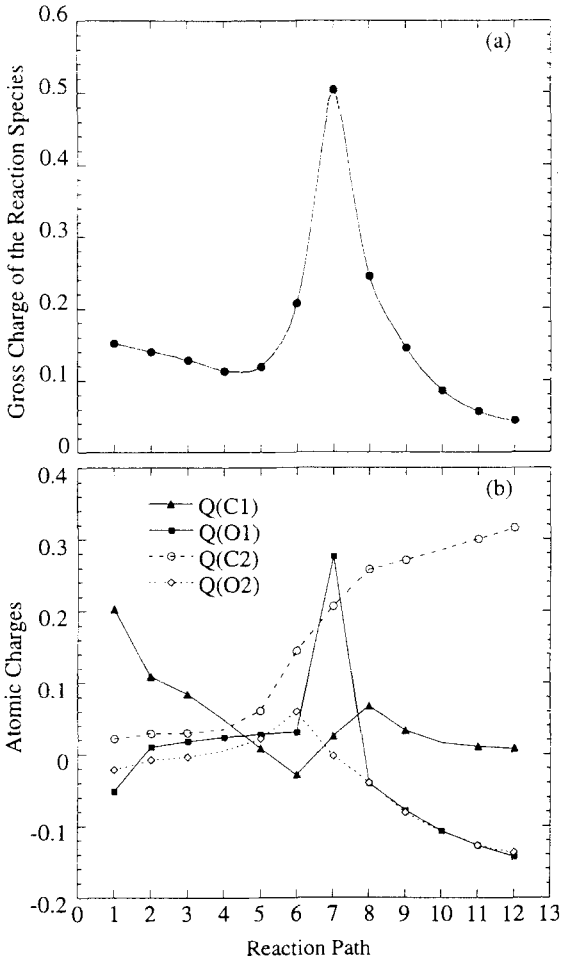

Figure 7. Mulliken population distribution along the reaction coordinate.

(a) Gross charge of the reaction species; (b) atomic charges of the reaction species. Here C1 and O1 are for the C and O atoms of the gas-phase CO and C2 and O2 for the C and O atoms of the adsorbed CO.

Steam-carbon reaction

We also performed similar minimum energy path calculations for the steam-carbon reaction on the FeO(100) surface. Here, the reaction coordinate is defined as the distance between the center of mass of H_2 and the surface plane for the forward reaction and the bond length of CO for the backward reaction. This procedure is shown in Figure 8. The minimum energy profiles calculated at both LSD and NLSD levels are displayed in Figure 9. Thermochemically, the calculation suggests that the steam-carbon reaction is an even steeper uphill process than the Boudouard reaction. Once again, the calculated activation barriers evaluated at both LSD and NLSD levels are extremely high, suggesting very unfavorable reaction kinetics.

We can similarly analyze the geometric change of the reaction species, and the charge transfer processes between the gas species and the surface along the reaction coordinate. The collected bond parameter changes of the reaction species are shown in Figure 10. Figure 10a displays the trajectory of the center of mass of H_2 from the surface: it gradually approaches the surface and leaves after going through the transition state. At the transition state, H_2 picks up the O atom to form H_2O, giving a steady distance between the center of mass of H_2 and O, as shown in Figure 10b. At relatively large separation, the CO bond is essentially unaffected by the in-

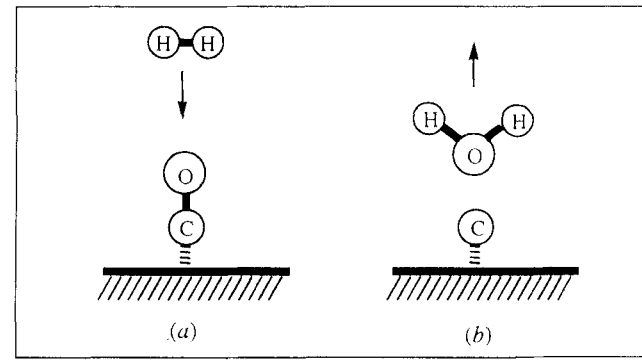

Figure 8. Reaction path calculations for steam-carbon reaction for normal incidence.

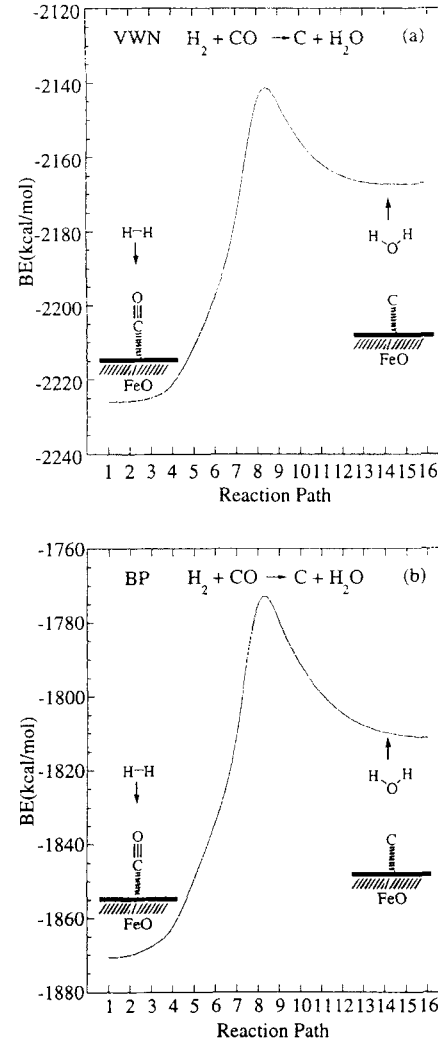

Figure 9. Energy profiles along the reaction coordinate of steam-carbon reaction calculated at: (a) LSD; (b) NLSD levels.

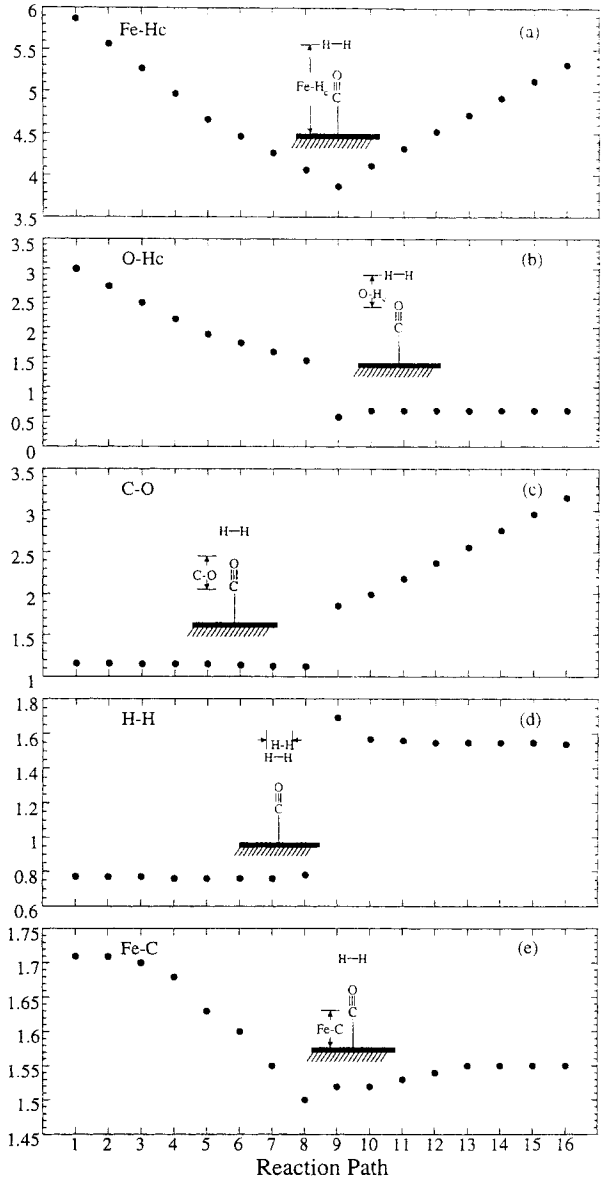

Figure 10. Structural changes along the reaction path of steam-carbon reaction for normal incidence.

(a) Distance between the center of mass of H_2 and the surface; (b) distance between the center of mass of H_2 and the O atom of the adsorbate; (c) bond distance of CO; (d) bond distance of H_2; (e) distance between the C atom and the surface.

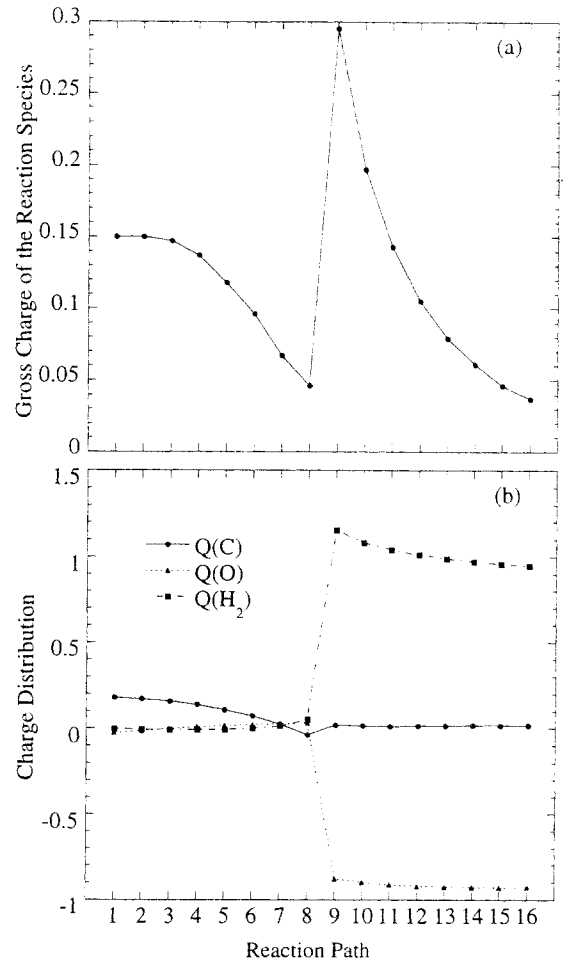

Figure 11. Mulliken population distribution along the reaction coordinate.

(a) Gross charge of the reaction species; (b) charge distribution of the reaction species.

coming H_2 until the transition state at which the bond is abruptly broken as suggested by Figure 10c. The sudden bond breaking is also clearly seen in Figure 10d. Here, the incident H_2 remains strongly bonded before the transition state and is abruptly broken at the transition state. Finally, Figure 10e shows the distance between C and the surface. It suggests that the adsorbate is initially compressed by the incoming H_2 and then forms a strong bond with the surface upon CO dissociation. The compressibility of CO on FeO(100) is understood since its adsorption on this surface is relatively weak.

The charge transfer process for the steam-carbon reaction is relatively simple. The gross charge of the reaction species along the reaction coordinate, shown in Figure 11a, is similar to that of the Boudouard reaction except for a more abrupt change at the transition state due to the sudden change of the bond dissociation and bond formation. The charge distribution of the individual reaction species is shown in Figure 11b. While the O atom gains charge upon the H_2O formation, H_2 loses electron to O upon the H_2 bond breaking. Finally, the behavior of the charge on C is similar to that in Boudouard reaction.

Orbital interactions

Our calculation suggests that all the electronic states near the Fermi level are contributed mostly by the surface states, which are primarily composed of the *d*-orbitals of the Fe atoms and the *p*-orbitals of the surface O atoms. The bonding states resulting from the orbital interaction between the adsorbate and the surface lie a few electron volts below the Fermi level. In particular, the interaction between the 5σ-orbital of CO, which is known to be slightly antibonding (Nakamoto, 1986), and the $4s$ and $3d_{z^2}$ orbitals of the adsorbing Fe atom gives rise to the adsorbate-surface bonding with electron donation from CO to the surface in nature,

which would strengthen the C-O bond of the adsorbate. On the other hand the orbital interaction between the 2π-orbital of CO and the d_{xz} and d_{yz} orbitals of the Fe atom results in electron back donation from the surface to the adsorbate. Since the 2π-orbital of CO is antibonding, the back donation would cause weakening of the C-O bond. Furthermore, the strong covalent Fe-O bonds of the FeO surface tend to remove the d-electrons from the Fe atoms toward the O atoms. Consequently, the electron back donation is limited. Indeed, the calculated gross charges of the reaction species indicate that the electron donation prevails over the back donation in this case; as a result, the C-O bond of the adsorbate is very strong. This explains the relatively weak bonding and the large compressibility of CO on FeO(100) and why C-O dissociation is difficult at the FeO(100) surface.

From a molecular orbital point of view, the normal incidence of CO and H_2 is also not a favorable process in optimal orbital overlap. The bonding σ-orbitals of the incoming molecules do not match the symmetry of the antibonding 2π-orbital of the adsorbate. We also examined the incidence from the angles that allow better orbital symmetry match between the incoming molecules and the adsorbate for both the Boudouard and steam-carbon reactions. The calculated results suggest that in both cases the reactions are not energetically favorable processes. The underlying reason is that the electron back donation from the surface to the adsorbate is too small to weaken the C-O bond for dissociation.

Summary

Density functional theory was used to investigate the possible cause of two major metal dusting processes represented by the Boudouard and steam-carbon reactions on the FeO(100) surface, with the focus on the underlying mechanisms that lead to the bond dissociation of CO and deposition of C on surfaces. The reason why transition metal oxides may minimize the dusting process is also explained.

This work utilizes cluster models to represent the FeO(100) surface. The utility of these models is validated by performing calculations for CO adsorption on various size clusters of FeO(100). A relaxation scheme for a given cluster needs to be carefully chosen to obtain consistent results while still resembling the bulk structure. It was found that lattice relaxation, while important, has a relatively small effect on the CO adsorption binding energy and is thus neglected in our calculations. The rigid lattice model has considerably reduced our computational effort. A direct abstraction process, in which a gas-phase CO reacts with an O atom of the surface, is an energetically unfavorable process.

The optimized CO adsorption structure on FeO(100) gives a relatively small adsorption binding energy. For both the Boudouard and steam-carbon reactions, we also performed minimum energy path calculations for normal incidence and for the incidence from different angles that allow orbital symmetry match between the adsorbate and the incoming molecules. It should be pointed out that for both the Boudouard and steam-carbon reactions, the gas-phase species can change their orientations freely without significant energy cost at large separation from the surface. However, the molecular orientations chosen for the incidence in both cases (Figures 4 and 8) are the only reasonable ones that may result in the reactions. The calculated minimum energy paths indicate that these reactions are extremely unfavorable both thermochemically and kinetically. The population analysis along the reaction paths provides detailed insight into the charge transfer processes in the gas-surface interface. The calculated electronic states and the population distribution suggest that the CO adsorption at the FeO(100) surface is dictated by the electron donation of the 5σ-orbital of CO to the $4s$ and $3d_{z^2}$ orbitals of Fe and the small back donation from the d_{xz} and d_{yz} orbitals of Fe to the 2π-orbital of CO. The calculations suggest that metal oxides are not catalytic accelerators for the Boudouard and steam-carbon reactions leading to metal dusting, thereby reducing the amount of carbon produced by these reactions on a given surface. We wish to point out that although the presented reaction paths seem to be the most natural ways leading to the metal dusting, other reaction paths may also exist. We have sampled a number of possible paths, such as dusting attack from nearby adsorbates, and found that they are not energetically favorable. The underlying reason is the weak adsorption of CO on the FeO(100) surface. Due to lack of $d \rightarrow 2\pi$ back donation, which results in relatively weak adsorption, the C-O bond is not sufficiently activated for the dusting reactions. Consequently, the adsorbate remains "inert" to the attack by either CO or H_2 regardless of whether the attack comes from the gas phase or from the adsorbing species.

Although this work dealt with the dusting phenomena only at the FeO(100) surface, the basic conclusions derived from it may also be applicable to other transition metal oxide surfaces. Based on the similar studies on NiO surfaces (Cheng, 1997) we concluded that both the Boudouard and steam-carbon reactions would be difficult due to the unfavorable energetics. This is consistent with the extensive studies in the literature on CO adsorption on surfaces of various metal oxides, such as MgO (Jug and Geudtner, 1996), TiO_2 (Linsebigler et al., 1995) and ZnO (Jaffe and Hess, 1995). In all cases, CO was weakly adsorbed on well aligned oxide surfaces, and chemisorption occurs only at surface defects and vacancies. CO can be readily activated at the defect/vacancy sites with a large adsorption energy and a considerably elongated bond (Cheng et al., 1997), which will ultimately lead to metal dusting. It should be pointed out, however, that this study mainly focuses only on one CO adsorption configuration, which appears to be the dominant adsorption pattern. Other configurations, while less energetically possible, may also be present in practice. In particular, the "side-on" adsorption on the surface may lead to much easier bond dissociation and thus facilitate the Boudouard and steam-carbon reactions. We will investigate the effect of various adsorption patterns on these reactions in a future study.

An important conclusion from this work is that in most cases the normal oxides present on stainless steel should prevent Boudouard carbon deposition. However, the presence of defects in these oxides will yield sites for local carbon deposition to occur. As a result, the attack should take the form of pits occurring at these local sites as carbon diffuses into the metal at these sites, ultimately causing the loss of metal from these sites. The observation of pitting attack as a result of metal dusting has not been adequately explained in the prior literature, but based on this work it is clear that pitting should be the preferred mode of attack. However, this work does

not explain the occurrence of crevice attack which is also often observed in metal dusting situations.

Acknowledgment

We gratefully acknowledge Drs. Carlos Valenzuela and John Pfeiffer for their support of this research.

Literature Cited

Becke, A. D., "Hartree-Fock Exchange Energy of an Inhomogeneous Electron Gas," *Int. J. Quan. Chem.*, **23**, 1916 (1983).

Cheng, H., D. B. Reiser, P. M. Mathias, K. Baumert, and S. W. Dean, Jr., "Investigation of Nitriding Mechanism at Transition Metal Surfaces: NH_3 Adsorption and Decomposition on Fe(100), Ni(100), and Cr(100)," *J. Phys. Chem.*, **99**, 3715 (1995).

Cheng, H., D. B. Reiser, P. M. Mathias, K. Baumert, and S. W. Dean, Jr., "Structures and Energetics of NH_3 Adsorption and Decomposition at Nb(100) Surface: A Density Functional Study," *J. Phys. Chem.*, **100**, 9800 (1996).

Cheng, H., R. M. Pearlstein, and D. Ramprasad, "Density Functional Study of Oxygen Sorption in Cyanocobaltate Complexes: Reversibility and Charge Transfer," *J. Phys. Chem.*, **100**, 17613 (1996).

Cheng, H., D. B. Reiser and S. W. Dean, Jr., "Implication of CO Adsorption on Transition Metal Surfaces to Metal Dusting," in press (1997).

Davis, W. R., R. J. Dlawson, and G. R. Rigby, "Unusual Form of Carbon," *Nature*, **171**, 756 (1953).

DMOL, v2.3.6, Biosystem Technologies, San Diego, CA (1994).

Ellis, D. E., J. Guo, H. P. Cheng, and J. J. Low, "Transition Metal Clusters: Electronic Structure and Interaction with Hydrogen and Oxides," *Adv. Quant. Chem.*, **22**, 125 (1991).

Estiu, G. L., and M. C. Zerner, "Icosahedral Symmetry and Magnetic Properties of Small Nickel Metal Clusters," *J. Phys. Chem.*, **98**, 9972 (1994).

Feiblman, P, "Making Sense of Surface Structure," *Surf. Sci.*, **299/300**, 426 (1994).

Göpel, W., G. Rocker, and Feierabend, "Intrinsic Defects of Titanium Dioxide(110): Interaction with Chemisorbed Oxygen, Hydrogen, Carbon Monoxide, and Carbon Dioxide," *Phys. Rev. B*, **28**, 3427 (1983).

Grabke, H. J., R. Krajak, and E. M. Müller-Lorenz, "Metal Dusting of High Temperature Alloys," *Werkstoffe und Korrosion*, **44**, 89 (1993a).

Grabke, H. J., R. Krajak, and J. C. Nava Paz, "On the Mechanism of Catastrophic Carburization: Metal Dusting," *Corrosion Sci.*, **35**, 1141 (1993b).

Hammer, B., K. W. Jacobsen, and J. K. Nørskov, "Role of Nonlocal Exchange Correlation in Activated Adsorption," *Phys. Rev. Lett.*, **70**, 3871 (1993).

Hammer, B., and J. K. Nørskov, "Why Gold Is the Noblest of All the Metals," *Nature*, **376**, 238 (1995).

Hoyt, W. B., and R. H. Caughey, "High-Temperature Metal Deterioration in Atmospheres Containing Carbon Monoxide and Hydrogen," *Corrosion*, **15**, 21 (1959).

Jansen, S. A., and R. Hoffmann, "Surface Chemistry of Transition Metal Carbides: A Theoretical Analysis," *Surf. Sci.*, **197**, 474 (1988).

Jaffe, J. E., and A. C. Hess, "*Ab Initio* Study of a CO Monolayer Adsorbed on the (1010) Surface of ZnO," *J. Chem. Phys.*, **104**, 3348 (1995).

Jug, K., and G. Geudtner, "Quantum Chemical Study of Carbon Monoxide Adsorption at the MgO(100) Surface," *J. Chem. Phys.*, **105**, 5285 (1996).

Kane, R. H., *Process Industries Corrosion—The Theory and Practice*, B. J. Moniz and W. I. Pollock, eds., Nat. Assoc. of Corrosion Engs., p. 45 (1986).

Kobayashi, H., and M. Yamaguchi, "*Ab Initio* MO Study of Adsorption of Carbon Monoxide Molecule on Titania Surfaces," *Surf. Sci.*, **214**, 466 (1989).

Koszman, I., *High Temperature Gas-Metal Reactions in Mixed Environments*, S. A. Jansson and Z. A. Foroulis, eds., Metall. Soc. of AIME, p. 155 (1973).

Labanowski, J. K., and J. W. Andzelm, *Density Functional Methods in Chemistry*, Springer-Verlag, New York (1991).

Linsebigler, A., G. Lu, and J. T. Yates, "CO Chemisorption on TiO2(110): Oxygen Vacancy Site Influence on CO Adsorption," *J. Chem. Phys.*, **103**, 9438 (1995).

Mijoule, C., Y. Bouteiller, and D. R. Salahub, "Density Functional Calculation of the Vibrational Stretching Mode of Carbon Monoxide Coadsorbed with Ammonia on Palladium Clusters," *Surf. Sci.*, **253**, 375 (1991).

Nakamoto, K., *Infrared and Raman Spectra of Inorganic and Coordination Compounds*, Wiley, New York (1986).

Neurock, M., R. A. van Santen, W. Biemolt, and A. P. Jansen, "Atomic and Molecular Oxygen as Chemical Precursors in Oxidation of Ammonia by Copper," *J. Amer. Chem. Soc.*, **116**, 6860 (1994).

Perdew, J. P., and Y. Wang, "Accurate and Simple Analytic Representation of the Electron Gas Correlation Energy," *Phys. Rev. B*, **45**, 13244 (1992).

Richardson, J. A., "Boudouard Carbon and Metal Dusting. (Steam Reforming Plants)," *Nitrogen*, **205**, 49 (1993).

Siegbahn, P. E. M., and U. Wahlgren, "A Theoretical Study of Atomic Oxygen Chemisorption on the Nickel(100) and Nickel(111) Surfaces," *Int. J. Quan. Chem.*, **42**, 1149 (1992).

van Daelen, M. A., Y. S. Li, J. M. Newsam, and R. A. van Santen, "Energetics and Dynamics for NO and CO Dissociation on Cu(100) and Cu(111)," *J. Phys. Chem.*, **100**, 2279 (1996).

van Santen, R. A., and M. Neurock, "Concepts in Theoretical Heterogeneous Catalytic Reactivity," *Catal. Rev.-Sci. Eng.*, **37**, 557 (1995).

van Santen, R. A., *Theoretical Heterogeneous Catalysis*, World Scientific, Singapore (1991).

Vosko, S. J., L. Wilk, and M. Nusair, "Accurate Spin-Dependent Electron Liquid Correlation Energies for Local Spin Density Calculations: A Critical Analysis," *Can. J. Phys.*, **58**, 1200 (1980).

Walker, Jr., P. L., J. F. Rakszawski, and G. R. Imperial, "Carbon Formation from Carbon Monoxide-Hydrogen Mixtures over Iron Catalysts," *J. Phys. Chem.*, **63**, 133 (1959).

Yates, Jr., J. T., "Chemisorption on Surfaces—An Historical Look at a Representative Adsorbate: Carbon Monoxide," *Surf. Sci.*, **299**, 731 (1994).

Ziegler, T., "Approximate Density Functional Theory as a Practical Tool in Molecular Energetics and Dynamics," *Chem. Rev.*, **91**, 651 (1991).

Manuscript received May 19, 1997, and revision received July 14, 1997.